**Atmospheric
Chemistry
and Physics**

Changes in the production rate of secondary aerosol particles in Central Europe in view of decreasing SO$_2$ emissions between 1996 and 2006

A. Hamed[1], W. Birmili[2], J. Joutsensaari[1], S. Mikkonen[1], A. Asmi[3], B. Wehner[2], G. Spindler[2], A. Jaatinen[1], A. Wiedensohler[2], H. Korhonen[1], K. E. J. Lehtinen[1,4], and A. Laaksonen[1,5]

[1]Department of Physics and Mathematics, University of Eastern Finland (University of Kuopio),
P.O. Box 1627, 70211 Kuopio, Finland
[2]Leibniz Institute for Tropospheric Research, Permoserstrasse 15, 04318 Leipzig, Germany
[3]Division of Atmospheric Sciences, Department of Physical Sciences, University of Helsinki,
P.O. Box 64, 00014 Helsinki, Finland
[4]Finnish Meteorological Institute, Kuopio Unit, P.O. Box 1627, 70210 Kuopio, Finland
[5]Finnish Meteorological Institute, P.O. Box 503, 00101 Helsinki, Finland

Abstract. In anthropogenically influenced atmospheres, sulphur dioxide (SO$_2$) is the main precursor of gaseous sulphuric acid (H$_2$SO$_4$), which in turn is a main precursor for atmospheric particle nucleation. As a result of socio-economic changes, East Germany has seen a dramatic decrease in anthropogenic SO$_2$ emissions between 1989 and present, as documented by routine air quality measurements in many locations. We have attempted to evaluate the influence of changing SO$_2$ concentrations on the frequency and intensity of new particle formation (NPF) using two different data sets (1996–1997; 2003–2006) of experimental particle number size distributions (diameter range 3–750 nm) from the atmospheric research station Melpitz near Leipzig, Germany. Between the two periods SO$_2$ concentrations decreased by 65% on average, while the frequency of NPF events dropped by 45%. Meanwhile, the average formation rate of 3 nm particles decreased by 68% on average. The trends were statistically significant and therefore suggest a connection between the availability of anthropogenic SO$_2$ and freshly formed new particles. In contrast to the decrease in new particle formation, we found an increase in the mean growth rate of freshly nucleated particles (+22%), suggesting that particle nucleation and subsequent growth into larger sizes are delineated with respect to their precursor species. Using three basic parameters, the condensation sink for H$_2$SO$_4$,

the SO$_2$ concentration, and the global radiation intensity, we were able to define the characteristic range of atmospheric conditions under which particle formation events take place at the Melpitz site. While the decrease in the concentrations and formation rates of the new particles was rather evident, no similar decrease was found with respect to the generation of cloud condensation nuclei (CCN; particle diameter >100 nm) as a result of atmospheric nucleation events. On the contrary, the production of CCN following nucleation events appears to have increased by tens of percents. Our aerosol dynamics model simulations suggest that such an increase can be caused by the increased particle growth rate.

1 Introduction

Aerosol particles play a key role in balancing the earth's radiation budget due to their light-scattering and cloud-forming properties (Haywood and Boucher, 2000) as well as through heterogeneous chemical reactions and the budget of photo-oxidants (Ravishankara, 1997). In regional and global scales, aerosol particles have a potential to change climate patterns and the hydrological cycle (Ramanathan et al., 2001; Sekiguchi et al., 2003; Lohmann and Feichter, 2005). A better understanding of these aerosol-related effects, especially with respect to long-term climate projections, requires a more comprehensive knowledge on the aerosol sources, and their atmospheric transformation processes. An important

process controlling the number concentration of atmospheric particles is the formation of new ultrafine particles typically 1–2 nm in size, through gas-to particle conversion (e.g. Kulmala et al., 2004a; Jeong et al., 2004). Once thermodynamically stable, the new particles can grow through condensation and coagulation to sizes of 50–100 nm where they become active light scatterers and cloud condensation nuclei (CCN). From numerous observations worldwide it is now evident that atmospheric aerosol formation followed by condensational growth may occur in almost any part of the troposphere (Kulmala et al., 2004b).

Sulphuric acid (H_2SO_4) is considered as the most important species contributing to atmospheric particle nucleation (Weber et al., 1999; Kulmala, 2003). Its concentrations in tropospheric air, however, are typically not sufficient to account for the observed growth of fresh nuclei to sizes larger than 10 nm (Birmili et al., 2003; Wehner et al., 2005). Exceptions have been reported for the sulphur-rich urban atmosphere of Pittsburgh (Stanier et al., 2004). Other condensable vapours have been concluded to participate in the growth of nano-sized clusters, such as the oxidation products of volatile organic compounds (VOCs). According to the current understanding, sulphuric acid is likely to trigger nucleation whereas the oxidation products of VOCs dominate the particle growth to larger sizes (Kulmala et al., 2007; Zhang et al., 2004; Laaksonen et al., 2008).

The major precursor of H_2SO_4 in the continental troposphere is sulphur dioxide (SO_2), which is oxidized during daytime by the hydroxyl (OH) radical. As a result of legislative emission control, the European levels of sulphur dioxide have undergone a substantial decrease over the last 2–3 decades (Manktelow et al., 2007; Beilke and Uhse, 1999). As a consequence of SO_2 reductions, the mass concentrations of sulphate aerosols have decreased as well (e.g. Spindler et al., 2004).

In the present work, our hypothesis is that the SO_2 reductions have also led to a reduced intensity of new particle formation and, consequently, to reduced number concentrations of secondary aerosols. In order to prove or disprove our hypothesis, we present two continuous data sets recorded in Melpitz, East Germany, during 1996–1997 and 2003–2006. Events of new particle formation are identified and characterized by their frequency, and the observed particle formation and growth rates. We furthermore examine the effects of sulphur dioxide and other parameters (in particular, solar irradiation and condensation sink) that have been shown to be influential on the occurrence of new particle formation in the continental boundary layer, and show that between the two periods examined, the reduction in SO_2 levels has indeed most likely caused the observed reduction in the production of freshly nucleated particles. Finally, the effects of changing SO_2 on the production of cloud condensation nuclei (CCN) following nucleation events are evaluated and discussed. This is done by both examining the observed particle growth into CCN size range as well as simulation of typical formation events for both time periods using the sectional aerosol dynamics code UHMA.

2 Methods

2.1 Experimental data

Ambient particle number size distributions as well as a number of meteorological and gas phase parameters have been recorded at the atmospheric research station Melpitz (51°32′ N, 12°56′ E; 86 m a.s.l.). The station is located near the village of Melpitz and about 46 km northeast from the city of Leipzig in Saxony (Eastern Germany). The region lies within densely populated central Europe, and is characterized by the presence of various anthropogenic sources, such as vehicular traffic, and agricultural and regulated industrial emissions. The surrounding of the station itself is flat grass land, where agriculture and wooded areas dominate up to a distance of several tens of kilometres around the station. The immediate neighbourhood of the station, however, is not used for agricultural purposes except grass being mowed once or twice a year. Details of the station can be found in Birmili and Wiedensohler (2000). Particle size distribution measurements were carried out using twin DMPS systems (Differential Mobility Particle Sizers) with particle size ranges of 3–750 nm at Melpitz station during both periods (1996–1997 and 2003–2006). The instrument consists of Hauke differential mobility analyzers (DMA) and TSI CPC 3010 and UCPC 3025 particle counters (Birmili et al., 1999). The first DMPS measures particle size distributions between 3–20 nm and the second one between 15–750 nm. One measurement cycle lasts for ten minutes. The same measurement technique and a very similar data processing method were used during both measurements periods. Two size distribution data sets are used in this work: March 1996–August 1997 and July 2003–June 2006. Some parts of these data sets were presented before, examining the environmental factors contributing to secondary new particle formation, the dependence of the particle size distribution on large-scale air masses, as well as the behaviour of the non-volatile particulate aerosol fraction (Birmili and Wiedensohler, 2000; Birmili et al., 2003; Engler et al., 2007). Our analysis also uses gas phase and meteorological parameters collected at the station, including SO_2, O_3, temperature, and global radiation. Table 1 summarizes all measured parameters, instruments, measuring ranges, and detection limits for different parameters at Melpitz station.

Gas phase and meteorological parameters from eleven observation sites were taken from routine observations by UBA (Federal German Environmental Agency, Dessau, Germany). All gas analyzers were regularly calibrated using calibration standards.

Table 1. Summary of measured gas and meteorological parameters, instruments, measuring ranges and detection limits at the Melpitz measurement station.

Parameter	Instrument	Measuring Ranges	Detection limit
SO_2	Monitor – APSA 360 UV-fluorescence, Horiba Europe	0–0.05/0.1/0.2/0.5 ppm	0.5 ppb+1%
NO_2/NO	Monitor – APNA 360 chemiluminescence Horiba Europe	0–0.1/0.2/0.5/1 ppm	0.5 ppb+1%
O_3	Monitor – APOA 350E, UV-absorption Horiba Europe	0–0.1/0.2/0.5/1 ppm	0.5 ppb+1%
Temperature	Pt 100/DIN 43760	−40 to +40 °C	+0.1 K at 0° C
Relative Humidity	Humidity sonsor	0–100%	+3% (20–95%)
wind speed	Cup Anemometer	0–40 m/s	+0.3 m/s
Wind direction	Wind vane type RITA	0–360°	+2°
Global radiation	Kipp & Zonen CM6	2000 W/m^2 (305–2800 nm)	

2.2 Nucleation event classification, and determination of condensation sink, and particle formation and growth rates

All days from the studied periods were classified into different categories, i.e., nucleation and non-nucleation days, depending on whether particle formation events were observed. During nucleation event days, an increase of the particle number concentration in the nucleation mode connected with a clear growth of the newly formed particles for several hours can be observed. If no formation of new particles has been observed, the day has been classified as non-nucleation day. If a day cannot be clearly classified as nucleation or non-nucleation day, it is classified as an "equivocal case". The classification method of nucleation events we used here is based on the method described in Hamed et al. (2007). In the resulting analysis and to minimize the uncertainty of the classification subjectivity, only the clear nucleation events and non-events were taken into consideration.

The aerosol condensation sink (CS) determines how rapidly molecules are scavenged by condensation onto pre-existing aerosols and depends strongly on the ambient particle size distribution. To quantify condensation processes during new particle formation, we calculated the condensation sink by using the method described by Pirjola et al. (1998) and Kulmala et al. (2001). In practice, the vapor was assumed to have very low vapor pressure at the surface of the particle, and its molecular properties were assumed similar to those of sulphuric acid. The condensation sink is closely related to the coagulation sink, which is an important loss term for clusters and small particles coagulating (mainly) with larger particles.

From the DMPS data, we calculated the formation rate of 3 nm particles (J_3) following the method described by Sihto et al. (2006) and Riipinen et al. (2007). The growth rates of the nucleation mode were estimated by following the nucleation mode peak evolution from daily size distribution contour diagrams. When quantifying the growth rate (GR) of the nucleation mode, a minimum growth time of three hours was required. If a continuous growth of the nucleation mode occurred, GR was estimated from periods lasting up to eight hours (Hamed et al., 2007).

2.3 CCN estimates from measurement data

In order to determine the production rates of CCN resulting from nucleation and growth of new particles, we applied the method of Laaksonen et al. (2005) to the size distribution data. Briefly, we calculated increases of particle number concentrations in the 50–750 nm, 100–750 nm, and 200–750 nm size ranges on nucleation event days. The concentration increases in the given size ranges were simply determined from the differences in particle concentration at the moment when the nucleated mode reaches lower limit of the given size range, and at the time when the particle concentration in that size range reaches a maximum, or alternatively at 06:00 h LT of the following day if a maximum was not reached before. The termination of the calculation at this point is a practical necessity because of the interferences created by the morning rush-hour aerosol and by the start of vertical mixing. In this way we obtain estimates for the increases of particle concentrations in the different size ranges. Quite similar techniques for determining CCN increases after nucleation have been used by Kerminen et al. (2005) and Kuang et al. (2009), with the main difference that they started their calculations from

Table 2. Particle emission parameters used for estimating the CCN production from primary mass emissions. d_{p1} and d_{p2} refer to the geometric mean mass diameters of the two particle modes, the values were converted to number GMDs by assuming unity density. M% is the assumed fraction of emitted mass in the smaller mode. The ranges given are estimates of typical range of values in literature. EMEP sector 7 is "Road Transport", sector 1 is "Combustion in energy & transformation Industry", sectors 2–6 contain manufacturing, industrial combustion, solvent use and fuel extraction emissions, and sectors 8–10 contain agriculture, mobile sources, waste treatment and other sources.

Emission source	d_{p1} (nm)	d_{p2} (nm)	M (%)	EMEP sector(s)
Traffic*	70 (30–120)	430 (400–1000)	5 (3–8)	7
Energy production**	90 (40–100)	430 (400–600)	3 (1–88)	1
Manufacture***	100 (80–110)	430 (400–600)	1 (0.5–2)	2–6
Other****	30 (20–50)	850 (500–1500)	0.1 (0.01–0.5)	8–10

* Based on diesel exhaust data Morawska et al. (1998).
* Ohlström et al. (2000)
** Extrapolated from Figs. 3 and 12 in Ehrlich et al. (2007).
*** Other mobile emissions and agricultural emissions.

the nucleation event start rather than from the time when the nucleation mode first reached the size range in question.

In order to estimate the total CCN production, i.e. the production from primary and secondary sources, we calculated hypothetical particle source rates that are needed to support the average concentrations of particles in the given size ranges. In the steady state (SS), the particle source rate (P) equals the ratio of particle concentration (C) and the average particle residence time in air (*t*). For our calculations we adopted the residence time of 4 days for particles near the surface given by Balkanski (1991).

2.4 Estimate for CCN production from primary sources using emission inventory

To estimate the primary CCN production in a given area, existing emission inventories has been used. The accuracy of emissions inventories are for this application, however, limited since they usually refer to particle mass rather than particle number, and typically include only sources that have been officially reported. Further limiting factors include the lack of longer time-periods, seasonal variations and detailed size distributions and chemical composition of the particulate emissions. A further uncertainty is produced by the changes in the technology used to produce these mass emissions in the time period of this study, creating different number size distributions with the same mass emission rates. We expect, however, that the primary CCN emission rates can be estimated within order of magnitude on the basis of emission inventories.

The EMEP (European Monitoring and Evaluation Programme) emission model database provides estimates of annual emissions of $PM_{2.5}$ on 50×50 km grid cells for the years 2000–2005 (Vestreng et al., 2006, 2007). We created a rough estimate of the primary emitted CCN for the 2003-06 period by using these data and the source distributions of the

emissions. The estimate is based on the economic sectors of emissions from the EMEP database and typical literature distributions of different sources. For the years 1996 and 1997, with no specified EMEP emission model result available, we extrapolated the rates from year 2000 emission rates together with the trend of total $PM_{2.5}$ emissions in Germany from 1996 to 2000. One of our central assumptions was that the $PM_{2.5}$ emissions from different economic sectors represent, on average, a bimodal particle size distribution. In a first step, we distributed the mass emission to the two modes by a fixed (source-dependent) factor. Then the total modal particle number was calculated assuming a log-normal distribution leading to

$$N = \frac{6\,m}{\rho\pi}\mathrm{d_p}^{-2}\exp(-4.5\log^2\sigma)$$

where N and m are the total number and mass of the emission in the size and source mode ($\mathrm{m^{-2}\,year^{-1}}$ and $\mathrm{kg\,m^{-2}\,year^{-1}}$), d_p is the geometric mean number diameter (or count median diameter, CMD) of the emission (m), ρ is the effective density of the particles emitted ($\mathrm{kg\,m^{-3}}$), and σ is the geometric standard deviation of the emission mode. After this, the resulting number emission modes were summed up to a total emission size spectrum, which in turn was integrated to specific size ranges if needed. For the comparison with volume sources, the estimate of yearly area source of CCN from primary emissions is then multiplied by the presumed annual average height of the mixed layer in Melpitz site, 1 km in this case.

Table 2 describes the different emission categories we have used and the related factors used in estimating the number emission profiles. For traffic emissions (EMEP SNAP sector 7), we used an average number size distribution derived from diesel vehicles at maximum power (Morawska et al., 1998), resulting in CMDs of 70 nm and 430 nm with a relative mass ratio of 5% for the smaller CMD mode. For

non-traffic emissions, we first assumed that EMEP sector S1 (energy production) can be represented by coal combustion plants with CMDs of 90 nm and 430 nm with mass ratio of 3%, sectors S2 to S6 with mixed process plants with CMDs of 100 nm and 430 nm with mass ratio of 1% (extrapolated from Ehrlich et al. 2007, Figs. 3 and 12, and remaining sectors (other mobile emissions and agricultural emissions) were assumed to be unimodal coarse emissions with CMD of 5 μm. The values of these parameters do differ significantly in the literature (due to different measurement methods, technological differences and differing fuels), and so we decided to also use a representative range of values, together with the values above, from the literature for the values in traffic and energy production emission factors. For the other factors, we assumed similar ranges as in the energy production. The ranges of values used are indicated in the Table 2. In line with the very general nature of this analysis, we assumed that all the emission modes are constant in time and space, log-normal in shape with geometric standard deviation of 1.7 and no dynamic aging of emissions were considered. The particle density was assumed to be 800 kg m^{-3} for traffic-derived particles and 1500 kg m^{-3} for all other particles.

2.5 Estimate for CCN production using an aerosol microphysical model

We also estimated the contribution of NPF and primary sources to CCN in typical 1996/1997 and 2003/2006 conditions using an aerosol microphysical box model UHMA (Korhonen et al., 2004), which has previously been used in several studies of atmospheric new particle formation (Grini et al., 2005; Tunved et al., 2006; Komppula et al., 2006). The aerosol size distribution was described with 50 size bins in the range of 3 nm to 1.5 μm. The standard set-up of UHMA simulates the evolution of the aerosol population due to (1) nucleation via binary mechanism of H_2SO_4 and H_2O (Vehkamäki et al., 2002), ternary mechanism of H_2SO_4, NH_3 and H_2O (Napari et al., 2002), or kinetic or activation nucleation (Sihto et al., 2006), (2) condensation of sulphuric acid, low-volatile organic compounds and water, (3) coagulation, and (4) dry deposition. However, in the modified model version used in this study, we gave observed new particle formation (J_3) and growth rates (GR) as model input, and neglected dry deposition.

2.6 Statistical significance of the differences between the two measurement periods

In order to test for statistical significance of the differences between the two measurement periods, statistical analyses were carried out with R-software (R Development Core Team, 2008, see http://www.R-project.org) and the differences were tested with two sample t-tests. Since the observations are mostly not normally distributed, which is the conservative assumption for t-test to be valid; the results were

confirmed with robust Wilcoxon rank sum tests. Since the 1996–1997 data covers only a period of 1.5 years (with two summers and one winter), we did not compare the complete datasets with each other but instead present seasonal comparisons.

3 Results and discussion

3.1 Trends in atmospheric constituents

3.1.1 Sulphur dioxide (SO$_2$)

During the past twenty-five years European sulfur emissions have decreased continuously. The emission trend, however, varied considerably between individual countries. In the United Kingdom, France and Germany, particulate sulfate mass concentrations decreased by 50–70% between 1980 and 2000 in response to 90% reductions in emissions and measured concentrations of SO$_2$ (Manktelow et al., 2007; Lövblad et al., 2004). Germany, in particular, is a good example how industrial and domestic sulfur dioxide emissions were reduced according to the emission control polices (Gothenburg Protocol): The emissions decreased by 18% between 1980 and 1989 and by 85% between 1990 and 1999 (Beilke and Uhse, 1999; Elbet et al., 2000; Vestreng et al., 2007). It is essential to note that the decrease in East German emissions after 1989 can be largely ascribed to the de-industrialization process after Germany's reunification (Lintz et al., 2005). Since 2001, the national government has also encouraged the consumption of low-sulfur fuel in the road transportation by a tax discount. In East Germany the main pollution sources were associated with carbo-chemical industry (i.e. chemical industry based on processing lignite, brown coal as a raw material) as well as unregulated power plants. These industries clustered in the areas around Halle, Leipzig, and Cottbus, and therefore the Melpitz research station was erected in 1991 with the aim to monitor mid-term changes within this region. In the 1980s the contribution of power plants to total ambient SO$_2$ was 75%, which doubtlessly enhanced the formation of acidic secondary aerosols (Marquardt et al., 1998; Krüger et al., 2004). In the late 1980's, average SO$_2$ and PM mass concentrations of more than 150 μg m^{-3} were measured around Leipzig, Halle and Cottbus. After 1990, the SO$_2$ levels at these locations decreased to ca. 5 μg m^{-3} and PM levels to 20–30 μg m^{-3} (Spindler et al., 2004). The last "dirty" carbo-chemical plant in the Leipzig region (Espenhain works), dedicated to the pyrolysis of lignite, closed in late 1996.

In general, the reduction of emissions in the majority of European countries between 1990 and 2004 was more than 60%, while it was over 80% for a quarter of the countries (Vestreng et al., 2007). The absolute reductions obtained between 1990 and 2004 were the largest for Germany, the Russian Federation, UK, and Ukraine. The estimated reduction

within these four countries was larger than the reductions from all the other European countries together.

Myhre et al. (2004) showed that emission changes of SO_2 between 1985 and 1996 impacted the geographical distribution of the radiative forcing of the direct aerosol effect substantially. Krüger et al. (2004) showed that toward the late 1990s, the PM and SO_2 emission reductions in Central Europe (particularly in East Germany and in Poland) caused a reduction of the indirect aerosol effect and therefore of the cloud reflectance. Fagerli et al. (2006) showed that the reductions have a pronounced impact on the sulphur deposition pattern in Europe although SO_2 emissions have been reduced substantially since the 1980s. Further reductions are planned to help reduce fine particulate matter mass concentrations in Europe, which have been linked to adverse health effects.

The trend in sulfur dioxide concentrations was determined on the basis of local measurements at Melpitz. Figure 1a shows SO_2 trends measured at Melpitz as well as regional measurement stations near Melpitz between 1991 and 2008. The series are 60 day floating averages of daily average values between 10:00 and 14:00 h. The Melpitz values appear to be well representative of the regional SO_2 background. The Data were obtained from the German Federal Environment Agency (UBA) network.

Figure 1b shows monthly averaged SO_2 concentrations measured in Melpitz for the periods 1996–1997 and 2003–2006 (these periods cover our particle size distributions measurements). As indicated also by Fig. 1a, the SO_2 levels appear to have decreased between the two periods, in concurrence with the results of Vestreng et al. (2007). The overall reduction between averages from the two periods is 65%.

3.1.2 Nucleation event frequency and particle formation rate

Figure 2a shows the monthly average frequency of nucleation event days during the 1996–1997 and 2003–2006 periods. The results show in general that in the earlier dataset (1.5 years) 50% of the measurement days were nucleation days whilst only 30% were such in the newer dataset (2003–2006). Non-nucleation days accounted for 39% of the days in the earlier dataset and for 54% in the new one. Equivocal cases, i.e. days for which we were not able to decide with confidence whether nucleation took place or not, accounted for about 11% and 16% of the old and new datasets, respectively. From the event frequency plot, it is clearly seen that the highest frequencies for nucleation events in 2003–2006 were observed from late spring to late summer, i.e. from June till September while in 1996–1997 the maximum frequency was 80% in June. In wintertime (Dec-Feb) there were only a few nucleation events, with an average event frequency of ~10% for 1996–1997 and ~3% for 2003–2006. The total decrease in the numbers of nucleation days from years 1996–1997 to years 2003–2006 was about 45%. Figure 2b shows the 3 nm particle formation rate (J_3) determined for

the particle formation events. For the older data series the formation rate values were clearly higher than for the 2003–2006 data series. The relative difference of average J_3 values between the two periods was about 68%. Moreover, we examined the nucleation mode particle number concentrations for both datasets. The reductions in the number concentrations are of similar magnitude as the reductions in the formation rates (see Fig. 2c).

Table 3 shows the mean, median, standard deviation and p-values of the t-tests and Wilcoxon rank sum tests presented for the seasonal data. Note that the data are from strong nucleation event days only. The daily observations are from 06:00 a.m. to 06:00 p.m. The difference in the mean values is statistically significant if the p-value is below 0.05. Both tests indicate statistical significance for the differences of J_3 in spring, summer and autumn. Due to the scarcity of data and large standard deviations, the Wilcoxon test does not indicate the winter means of J_3 to be statistically different.

The annual event frequency can be biased by the weather conditions in a particular year. The solar radiation levels are a good measure for the differences between the years from nucleation point of view as photochemical reactions drive the formation of condensable species needed for nucleation to occur (Stanier et al., 2004; Birmili and Wiedensohler, 2000; Wehner and Wiedensohler, 2003; Hamed et al., 2007). We have therefore scrutinized both measurement periods for any meteorological differences by comparing the measured intensity of solar radiation (SR). Figure 3a shows the comparison of the radiation intensity between the two periods. No significant difference in SR is apparent during the months of highest nucleation event frequency (spring and summer) between the two periods. However, higher nucleation frequencies and rates in 1996–1997 may have been somewhat affected by more sunny weather in the winter months, whereas during the autumn months the 2003–2006 nucleation frequencies and rates may have been relatively more boosted.

The condensation sink (CS) for sulfuric acid and other condensable gases can have a preventing influence on nucleation and subsequent growth. Figure 3b shows CS in different seasons for both time periods. It can be seen that CS was higher in 1996–1997 during spring and summer whilst no remarkable difference is apparent in winter and autumn in the afternoons. As nucleation is much more frequent in spring and summer compared with autumn and winter, the CS may have diminished the differences in nucleation frequencies and rates going from 1996–1997 to 2003–2006.

The condensation sink differences are statistically significant for all seasons, while the solar radiation differences are significant only in autumn.

3.1.3 Sulphuric acid

Sulphuric acid is an oxidation product of sulphur dioxide. It is generally thought of as the primary compound responsible for atmospheric nucleation although other species such as
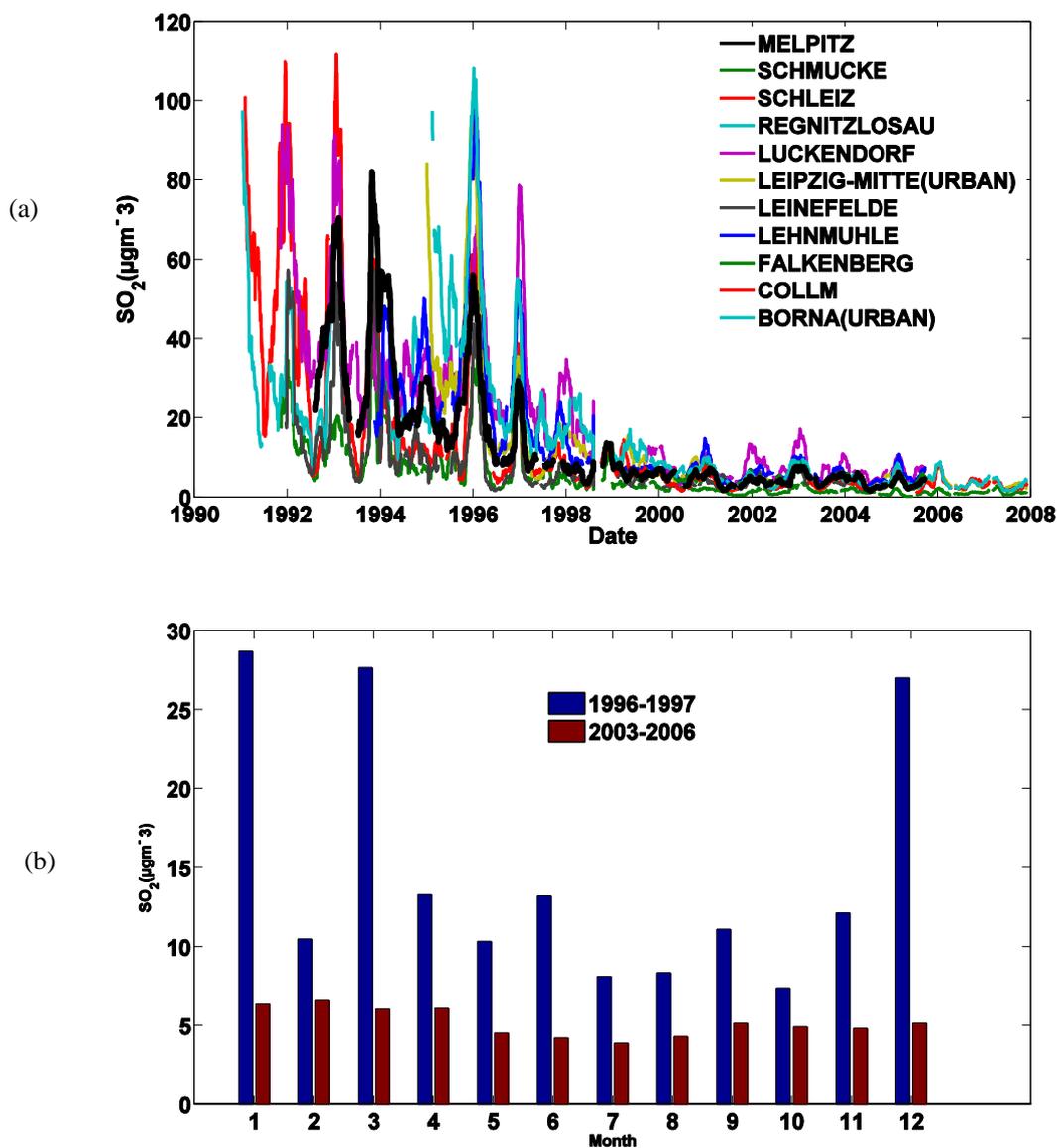
Fig. 1. (a) Measured SO_2 concentrations at Melpitz (black solid line) and some regional stations in the Leipzig area. The series are 60 day floating averages of daily average values between 10:00 and 14:00 h. The winter peaks in 1995/1996 and in 1996/1997 are clearly regional within a radius of 200 km, since they occur at all sites due to similar meteorological conditions. There is no sign that the Melpitz values are not representative for the regional SO_2 background. **(b)** Monthly average SO_2 concentrations (μg m^{-3}) for Melpitz in years 1996–1997 (blue) and years 2003–2006 (brown).

water, ammonia and organics might be involved as well (Weber et al., 1999; Kulmala, 2003; Zhang et al., 2004; Laaksonen et al., 2008). Since direct measurements of gas-phase sulphuric acid have not been performed at Melpitz, we calculated a proxy instead. The limiting step for the formation of H_2SO_4 is the reaction of SO_2 with the OH-radical. It has been shown that atmospheric OH concentrations correlate well with solar UV radiation (Rohrer and Berresheim, 2006). As UV radiation has not been measured continuously at Melpitz, we used the global intensity of solar radiation (SR) as its proxy. The most important sink for gas-phase

H_2SO_4 is the surface of existing atmospheric aerosol particles, onto which H_2SO_4 molecules condense rapidly. It is the CS that determines the corresponding rate of mass transfer, and this depends on the size distribution of existing particles. Assuming that the formation and loss of the acid are in steady-state, we obtain a proxy for gas-phase sulphuric acid concentration given by [SO_2]*SR/CS (Kulmala et al., 2005).

As shown in Fig. 4a the SO_2 concentration values were clearly higher for the older than for the 2003–2006 data sets in all seasons – and with a remarkable difference in spring and summer. However, we should note that in winter times

Table 3. Trends in solar radiation (SR) (in $W\,m^{-2}$), the condensation sink parameter (CS) (in s^{-1}), sulfur dioxide (SO_2) mixing ratio (in $\mu g\,m^{-3}$), sulphuric acid proxy, and the particle formation rate (J_3) (in $cm^{-3}\,s^{-1}$) at Melpitz. The results show seasonally separated data for strong nucleation days. The observations cover 06:00–18:00 LT. Mean, median, standard deviation (SD) and p-values of the t-tests and Wilcoxon rank sum tests for the seasonal growth rate (GR) (in $nm\,h^{-1}$) values were calculated from monthly mean values. In cases with statistically significant differences between the periods (both P-values <0.05) the higher mean values are highlighted with bold font.

Season	Variable	Mean		Median		SD		P-values	
		96–97	03–06	96–97	03–06	96–97	03–06	t-test	Wilcoxon
Winter	SR	154	124	91	94	156	140	0.363	0.474
	CS	0.009	**0.012**	0.010	0.011	0.005	0.004	0.008	0.049
	SO$_2$	**23.6**	13.6	22.4	5.6	20.7	12.9	0.019	0.179
	proxy	**2.59E+05**	1.23E+05	1.10E+05	3.89E+04	3.51E+05	1.69E+05	0.047	0.156
	J$_3$	4.9	0.7	1.2	0.4	6.4	0.9	0.073	0.247
	GR	4.1	5.6	3.9	4.6	1.6	2.3	0.216	0.156
Spring	SR	439	444	460	476	227	231	0.764	0.772
	CS	**0.012**	0.009	0.010	0.008	0.007	0.005	<0.0001	<0.0001
	SO$_2$	**15.7**	6.1	8.7	5.2	18.1	3.1	<0.0001	<0.0001
	proxy	**7.07E+05**	3.88E+05	4.07E+05	3.19E+05	7.48E+05	3.01E+05	<0.0001	<0.0001
	J$_3$	**10.2**	1.5	3.5	1.0	12.9	2.0	<0.0001	<0.0001
	GR	5.0	**6.1**	4.2	5.2	2.6	2.3	0.020	0.003
Summer	SR	487	464	499	456	225	221	0.069	0.075
	CS	**0.011**	0.009	0.010	0.008	0.006	0.006	<0.0001	<0.0001
	SO$_2$	**16.8**	3.8	10.3	3.4	18.5	2.7	<0.0001	<0.0001
	proxy	**6.88E+05**	2.47E+05	4.96E+05	1.85E+05	6.65E+05	2.52E+05	<0.0001	<0.0001
	J$_3$	**7.4**	1.8	2.7	1.0	9.7	2.2	<0.0001	<0.0001
	GR	5.9	**7.0**	5.1	6.4	3.2	2.8	0.025	0.002
Autumn	SR	258	**326**	253	331	204	203	0.017	0.013
	CS	0.009	**0.011**	0.008	0.010	0.003	0.008	<0.0001	0.054
	SO$_2$	**13.8**	4.7	6.9	4.1	16.8	3.6	<0.0001	<0.0001
	proxy	3.73E+05	2.07E+05	1.29E+05	1.50E+05	5.73E+05	2.17E+05	0.063	0.565
	J$_3$	**6.5**	2.0	3.0	1.0	7.9	2.8	0.033	0.017
	GR	5.6	6.4	5.0	6.0	2.9	2.3	0.474	0.334

the number of data points for SO_2 were not statistically significant (48 and 30 data points for years 1996–1997 and 2003–2006 respectively; see Table 3). Figure 4b shows that the proxy values have decreased concurrently with SO_2, and changes in SR and CS clearly do not explain this decrease (with the possible exception of autumn differences; see Table 3). We therefore conclude that the reduced sulphur dioxide levels not only coincide with but are the cause of the decreased sulphuric acid proxy values.

According to the t-test, the differences for SO_2 and the proxy are significant for all seasons (except for the autumn proxy), while the Wilcoxon test shows statistical significance for spring and summer only. As with nucleation rate, the small number of winter observations explains the Wilcoxon test result. In autumn, the Wilcoxon test does show significant difference for SO_2 but (as with the t-test) not for the proxy. This is caused by solar radiation, which was significantly higher in the 2003–2006 data, negating the effect of lowered SO_2.

As the decrease in the H_2SO_4 proxy is mostly caused by the observed decrease in SO_2, a corresponding decrease in the number of newly formed particles is expected if sulfuric acid is a critical species controlling the formation of new particles. Experimentally, the number of newly formed particles decreased between both periods as well (cf. Fig. 2a–b). However, it needs to be remembered that the precise balance of H_2SO_4 is influenced by further unknown variables, such as the concentrations of the OH radical.

A modelling study of new particle formation events in Pittsburgh suggested that SO_2 reductions can either increase or decrease the frequency of nucleation (Gaydos et al., 2005). They suggested that reductions of sulphur dioxide and the resulting sulphate by up to 40% actually increase the frequency of nucleation events in summer. This was explained by decreasing sulphate concentrations allowing higher gas-phase ammonia concentrations and, since they assumed a ternary (sulfuric acid – ammonia – water) nucleation mechanism, ammonia concentrations appeared to be a limiting factor for the events. In wintertime they could not see such an effect;
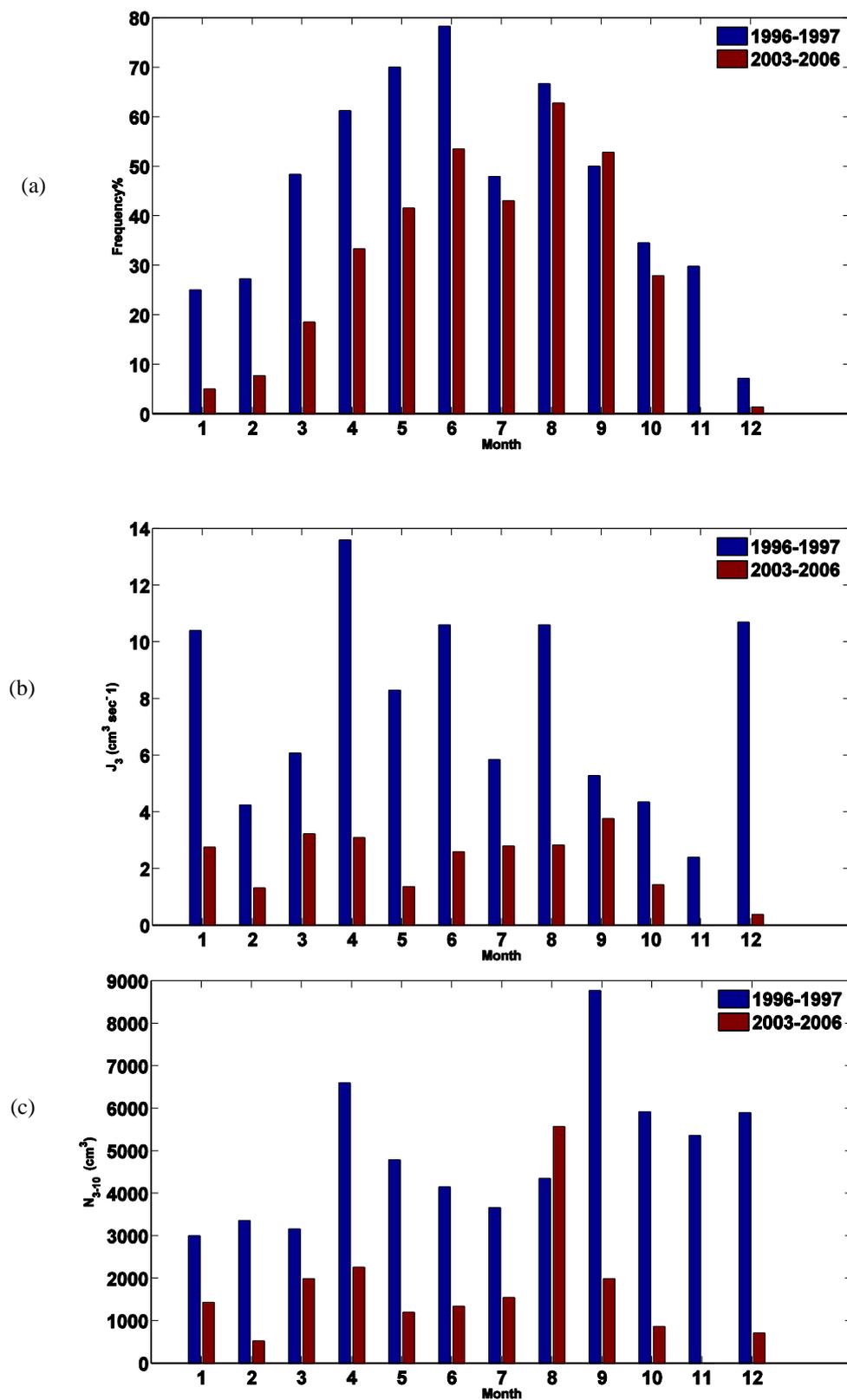
Fig. 2. Monthly average **(a)** frequency of new particle formation events, **(b)** the particle formation rate of 3 nm-particles (J_3) in ($cm^{-3} s^{-1}$) and **(c)** the nucleation mode particles concentrations 3–10 nm (cm^3) for the particle formation events in Melpitz in years 1996–1997 (blue) and years 2003–2006 (brown). In 2003–2006, no nucleation was observed in November, and only a few events were detected in December.
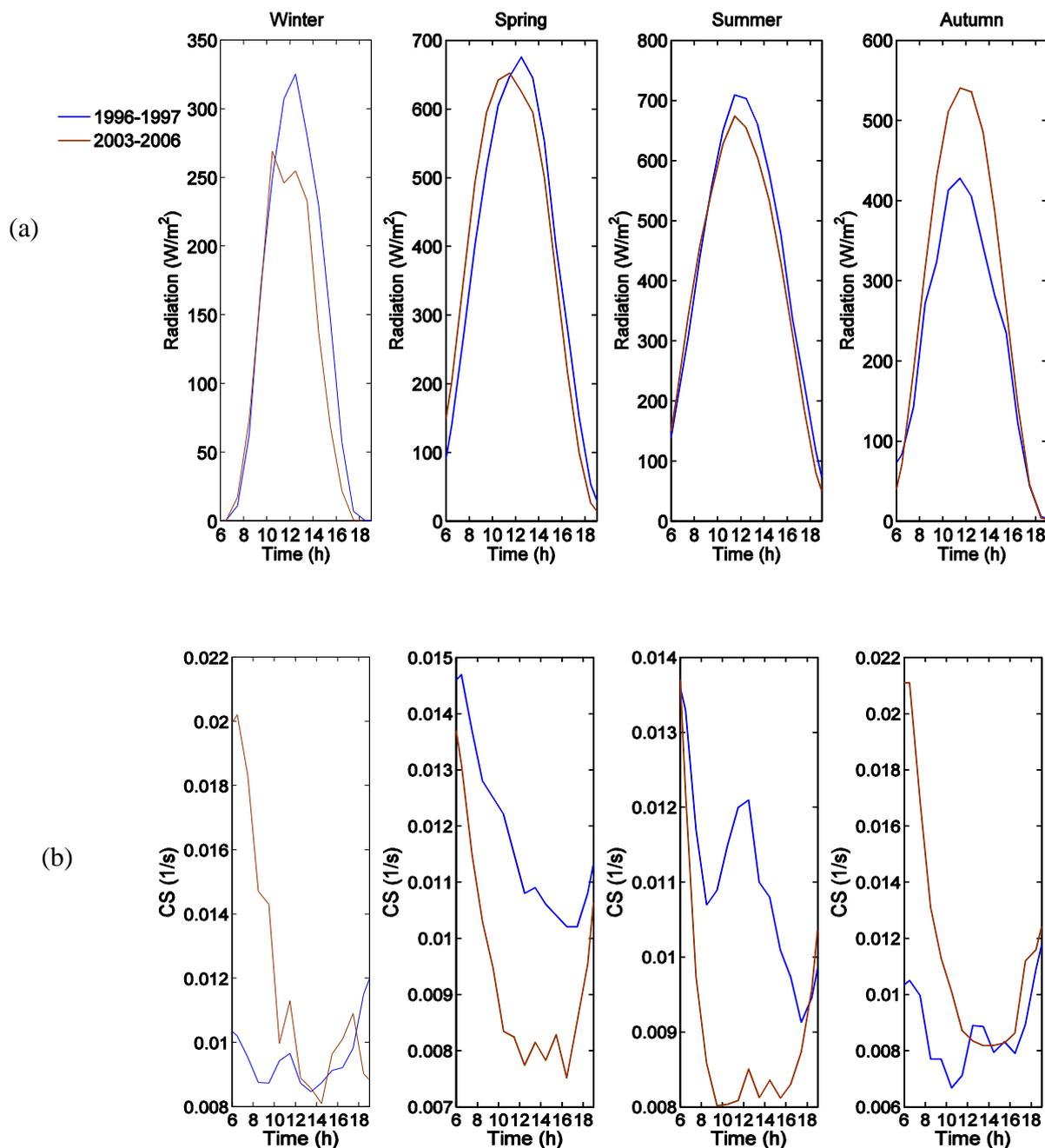
Fig. 3. Hourly average of **(a)** Global Solar Radiation "SR" (W/m^2) and **(b)** Condensation Sink "CS" (1/s) in different seasons for Melpitz 1996–1997 (blue) and 2003–2006 (brown).

the modelling predicted fewer nucleation events along with decreasing SO$_2$ concentrations (Gaydos et al., 2005). The field measurement study of new particle formation in clean area, Hyytiälä measurement station in Finland, found there were no correlations between SO$_2$ level and new particle formation (Boy and Kulmala, 2002; Lyubovtseva et al., 2005).

3.1.4 Particle growth rates

In contrast to the experimental particle formation rates, the growth rates of the fresh particles to bigger sizes increased by roughly 22% from 1996–1997 to 2003–2006. Growth rates were higher in 2003–2006 (see Fig. 5a) and the difference was statistically significant in spring and in summer (see Table 3). Therefore, the mean particle growth rate has increased
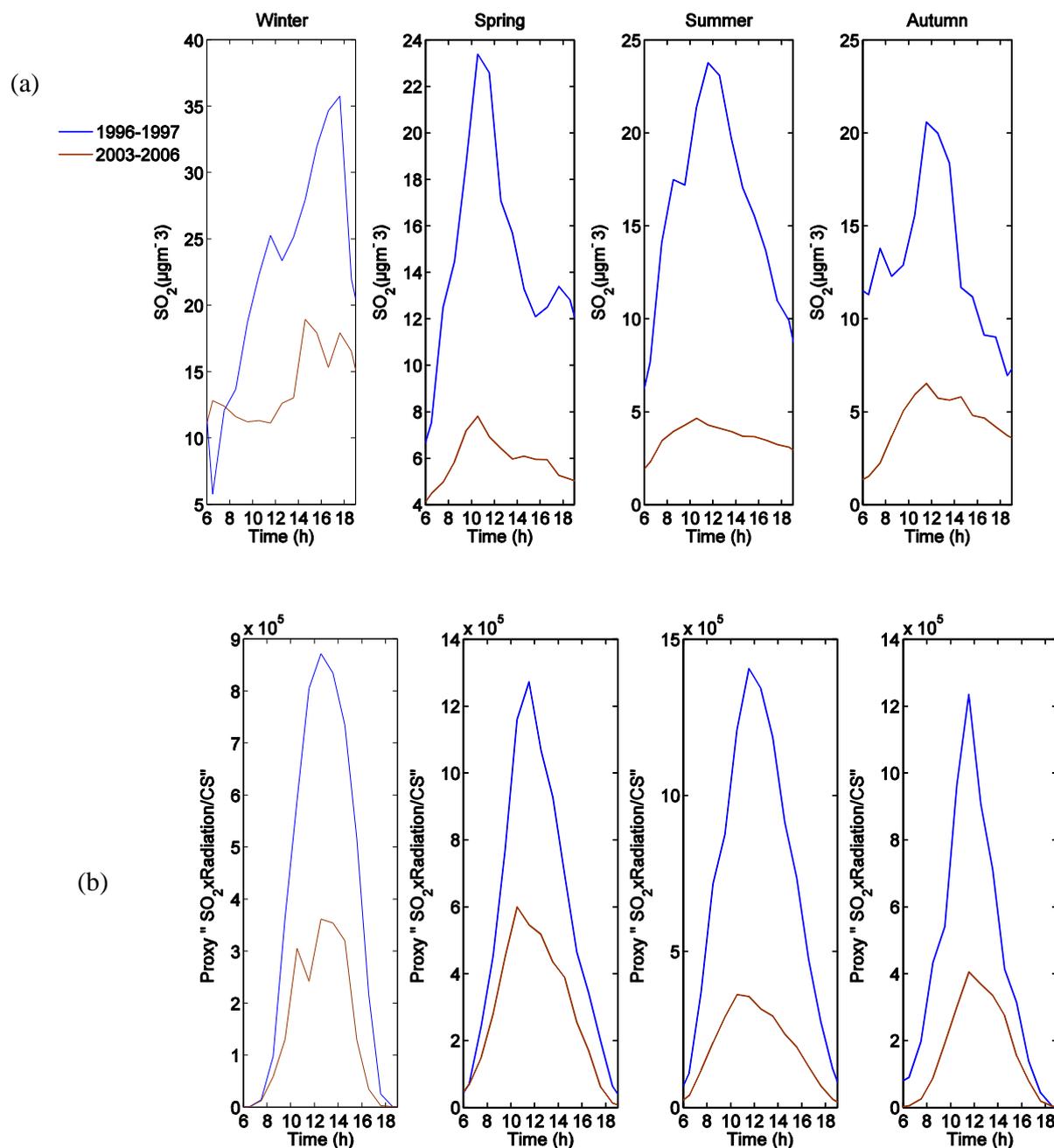
Fig. 4. Hourly average of **(a)** SO$_2$ concentration (μg m^{-3}) and **(b)** sulfuric acid proxy (product of SO$_2$ concentration and global radiation divided by condensation sink) in different seasons for Melpitz 1996–1997 (blue) and 2003–2006 (brown).

inversely to SO$_2$ concentrations, the H$_2$SO$_4$ proxy, and the formation rate of new particles. This observation is a clear indication of other species than H$_2$SO$_4$ being involved in the particle growth (Kulmala, 2003). It has been indicated that monoterpene oxidation products drive the growth of freshly nucleated particles in boreal forest areas (Tunved et al., 2006; Laaksonen et al., 2008). VOCs are also abundant in Central Europe (Müller et al., 2002; Alves et al., 2006), and it is

likely that their low-volatile oxidation products contribute to particle growth (Wehner et al., 2005). The question whether VOC concentrations have increased over our observation period at Melpitz cannot be answered with certainty. Biogenic VOC emissions are temperature dependent, and as the average nucleation day temperatures in 2003–2006 were higher than in 1996–1997 (see Fig. 5b), it could be that oxidation products of biogenic VOC's have contributed to the increased
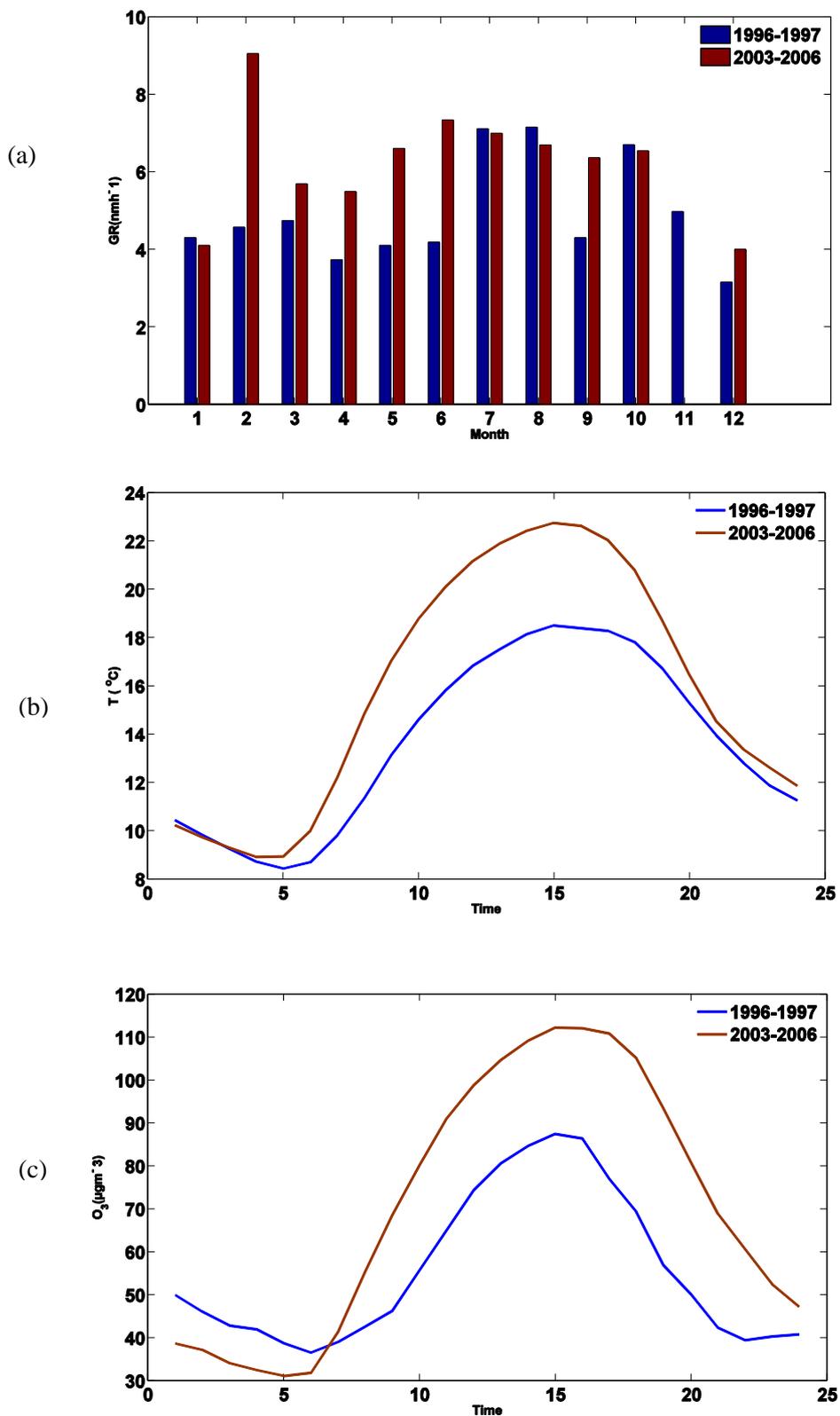
Fig. 5. (a) Monthly average of growth rate GR (nm h^{-1}) during particle formation bursts, hourly average of **(b)** temperature T ($^{\circ}$C) and **(c)** O$_3$ concentration (μg m^{-3}) at Melpitz in 1996–1997 (blue) and 2003–2006 (brown).

growth rates. Ozone is responsible for the formation of condensable species directly through reactions with VOCs, and indirectly by forming other oxidants (OH) upon photolysis. Although condensable organics might not be involved in the actual nucleation, they may be important in speeding up the growth of newly formed molecular clusters so that the clusters survive to detectable sizes before being scavenged by coagulation with larger particles (Kerminen et al., 2004). From our results we found that O_3 concentrations were higher on nucleation event days for new data sets than for old data (see Fig. 5c).

Industrial emissions of VOCs are expected to have decreased while traffic-derived emissions have slowly increased with time. A global estimate yielded that the SOA (secondary organic aerosol) production rate is currently rising (Heald et al., 2008). Note, however, that with decreased nucleation, the condensable vapour will be divided among fewer particles, and average growth rates could increase even if the condensable vapour levels stay constant. In this case even if condensable vapours from VOC oxidation have remained constant, the average growth rates might have increased.

3.2 Conditions and parameters of new particle formation

3.2.1 Separation of nucleation event and non-event days

The fact that the overall nucleation event frequency has decreased in line with the sulphuric acid proxy does not prove a causal relationship. We therefore examined the individual variables contributing to the H_2SO_4 proxy more closely with respect to their behaviour on nucleation event and non-event days. Figure 6 shows the production term ([SO_2]*SR) of the H_2SO_4 proxy as a function of the condensational sink (CS). Each point represents one day of measurements (in the case of formation events, at time when the maximum concentration of new particles formed by nucleation were reached; in case of non-events at noon). As can be seen, the data points from particle formation events and non-events tend towards different edges of the data cloud. The line that separates the two sub-sets most effectively is indicated in Fig. 6. The result illustrates that new particle formation at Melpitz becomes more probable when the ratio between the production term of the H_2SO_4 proxy and the CS increases. In contrast, the lower portion of the figure is dominated by non-nucleation days associated with comparatively low solar radiation, low [SO_2], or high CS, which all contribute to a low steady-state concentration of H_2SO_4. In conclusion, such a scatter plot of the sulphuric acid production and sink term appears to be an efficient illustration to explain a large part of the observed particle formation days, although the microphysical and meteorological understanding of the particle formation process is still missing. It is worth to note that a one-year study in
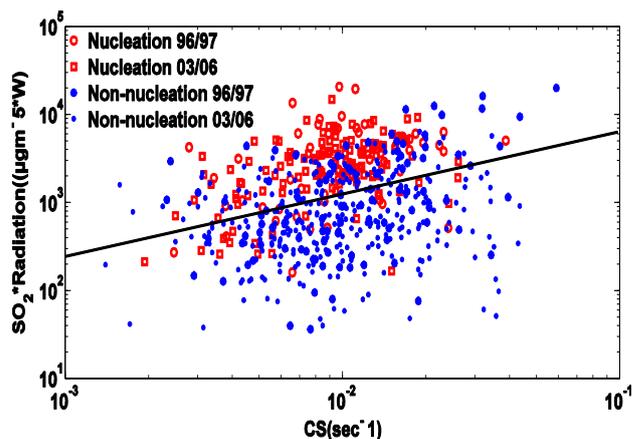

Fig. 6. The product of [SO_2] and solar radiation vs. condensation sink (CS) for particle formation events (red) and non-nucleation days (blue). In case of formation events, the parameters were calculated at time when the maximum concentration of new particles formed by nucleation were reached, in case of non-events at noon (12:00 LT). The separation line determined by discriminant analysis is given by Log_{10}([SO_2]*[Radiation])=4.52+0.709 Log_{10} (CS).

the urban atmosphere of Pittsburgh, Pennsylvania came to similar conclusions (Stanier et al., 2004).

3.2.2 Sulphuric acid proxy vs. nucleation rate

Figure 7 shows two examples of typical nucleation event days for both the old data period and for the new data period. The estimated 3 nm particle formation rates vs. the sulphuric acid proxy values are shown in the upper panels while the lower panels show the number concentration of 3–6 nm particles vs. the proxy. The sulphuric acid proxy was time delayed. This time delay between the rise in sulphuric acid proxy and particle number concentration N3–6 was interpreted as the time it takes for the clusters to grow from the nucleated size of 1 nm to the detectable size of 3 nm in diameter. Based on this assumption we used the growth rate (GR) to determine how long it takes for the clusters to grow from 1 nm to 3 nm for each nucleation day and therefore we estimated the delay time as 2 nm divided by GR. Figure 7 closely resembles similar plots e.g. in Sihto et al. (2006) with the difference that they show the daily behaviour of measured H_2SO_4 concentration instead of the H_2SO_4 proxy.

A plot of the logarithm of the experimentally derived particle formation rate J_3 vs. the logarithm of the sulphuric acid proxy reveals a rather scattered plot, resulting in weak correlation (see Fig. 8). Several studies have analyzed the slope of log (H_2SO_4) vs. log (J_3) because this could in principle reveal the number of sulfuric acid molecules required for a critical, thermodynamically stable cluster as well as give hints on the acting nucleation mechanism. Such studies have observed slopes between 1 and 2 (Eisele et al., 1997; Weber
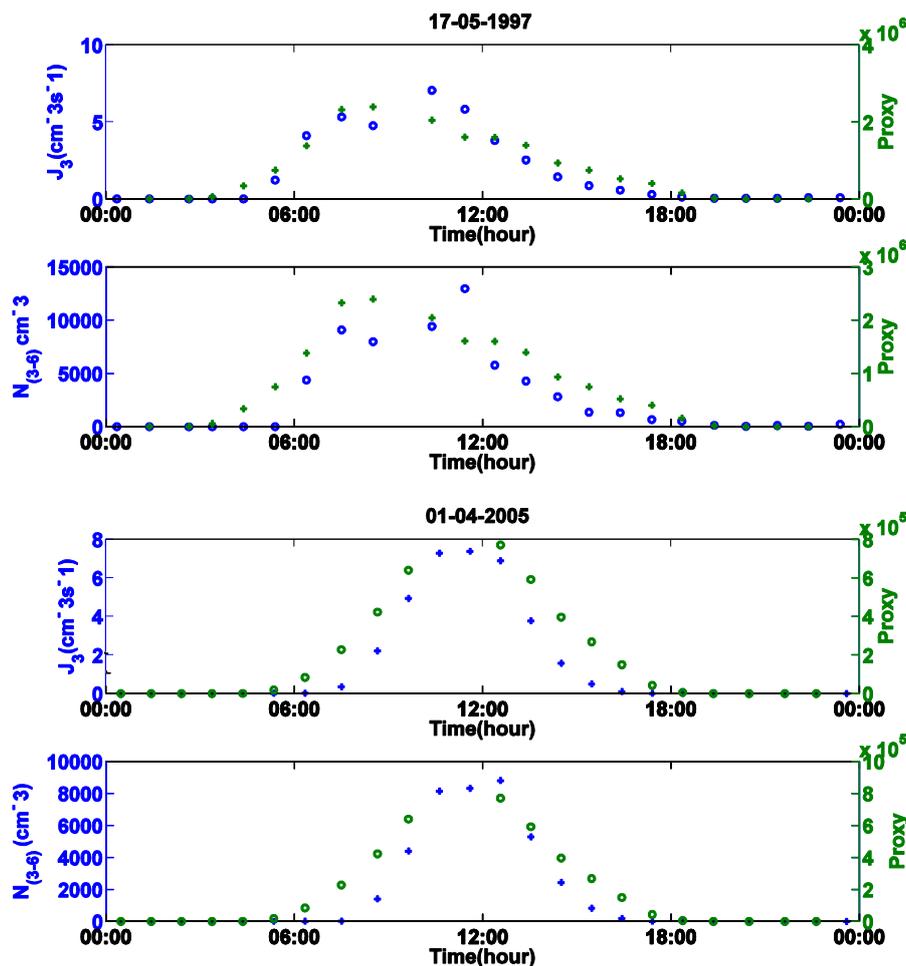
Fig. 7. Upper panels: The hourly averaged 3 nm particle formation rates (blue) versus the sulphuric acid proxy (green). Lower panel: The number concentration of 3–6 nm particles (blue) and the sulphuric acid proxy (green) on typical nucleation event days (17 May 1997 and 1 April 2005) in Melpitz for old data period and for new data period respectively. The proxy values have been shifted to the right in order to account for the time delay it takes for freshly nucleated particles to grow from 1 to 3 nm.

et al., 1999; Kulmala et al., 2006; Sihto et al., 2006; Kuang et al., 2008).

As seen from Fig. 8 the optimal fitted line shown has a slope of about one indicating reasonable consistency with earlier studies that investigated the relationship between J_3 and H_2SO_4. This result, together with Fig. 7, shows that our proxy variable behaves at least qualitatively similarly as H_2SO_4 which increases our confidence in interpreting the reduction of nucleation event frequency and nucleation rate between 1996–1997 and 2003–2006 as being due to reductions in sulfur dioxide emissions.

3.3 Implications for the production of CCN

After nucleating at diameters of about 1 nm in the atmosphere, the newly formed particles may grow by condensation and coagulation, and eventually reach particle sizes where they may act as cloud condensation nuclei (CCN).

This growth may take several hours to days, and since many aerosol dynamical as well as meteorological effects interact during such a time span, it has been difficult to determine CCN production rates on the basis of experimental observations. Here, we investigate the significance of the nucleation events as a source of CCN at Melpitz site, and whether the CCN production might have changed along with SO_2 concentrations. In the literature, CCN are defined either as particles activating to cloud drops at a given supersaturation, or alternatively (usually if CCN instruments were not available in the study) as particles larger than a given size. Here we examine three different size ranges: 50–750 nm, 100–750 nm, and 200–750 nm. The upper limit is set by the TDMPS instrument.

We examine three different CCN estimates. The first one is an estimate of CCN production by nucleation and subsequent growth. As explained in detail above, we follow the growing mode and calculate the CCN production from the increase in

Table 4. The annual yield of particles, the average yield per one nucleation event, the average particle concentrations and the hypothetical steady-state particle production rate at Melpitz during 1996–1997 and 2003-2006. To compare consistent annual mean values, we strictly selected a one year period (July 1996–June 1997) from the older dataset for our calculations.

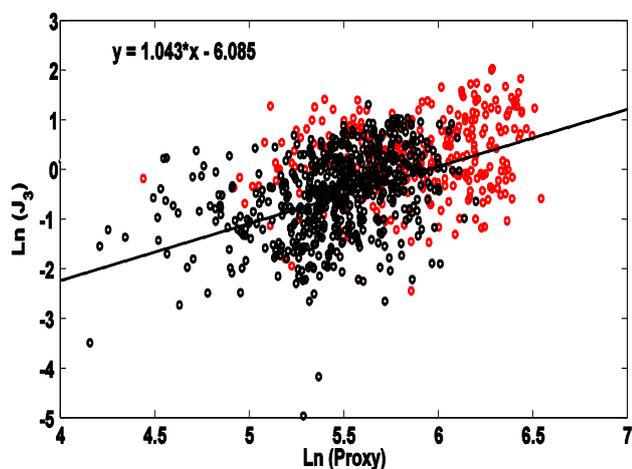|	1996–1997			2003–2006		
Size Range (nm)	50–750	100–750	200–750	50–750	100–750	200–750
Annual Yield/cc	2.29E+05	6.14E+04	1.56E+04	1.90E+05	9.00E+04	3.17E+04
Average Yield/Event	4.02E+03	1.08E+03	2.74E+02	3.61E+03	1.71E+03	6.03E+02
Average Concentration/cc	2.46E+03	1.20E+03	3.96E+02	2.43E+03	1.27E+03	4.38E+02
SS-Production/cc/Year	2.25E+05	1.09E+05	3.61E+04	2.22E+05	1.16E+05	4.00E+04

Fig. 8. The logarithm of 3 nm nucleation rate (hourly averages from strong nucleation event days between 06:00 a.m.–06:00 p.m.) versus logarithm of the sulphuric acid proxy. Melpitz 1996–1997 nucleation events (red) and (black) for Melpitz 2003–2006.

the number concentration into the given size range during the growth. The second estimate concerns total production (primary plus secondary) of CCN in the given size range, and is obtained from assuming a steady-state between particle production and removal that maintains the average concentration in the given size range, and a 4-day particle lifetime. The third estimate gives the numbers of primary CCN in the given size ranges, and is obtained from emission inventories for PM$_{2.5}$ plus assumed size distributions.

Note that all of the CCN estimates here contain more or less large uncertainties. The nucleation CCN estimate is interfered by air mass inhomogenities and by influences from other than nucleated particles that are difficult to tell apart, and by the need to terminate the calculation in the morning following the nucleation event. The total CCN estimate relies on a crude SS-assumption and on a 4-day particle lifetime. The primary CCN estimate relies on uncertain PM$_{2.5}$ numbers and on assumed size distributions and boundary layer height. We would like to stress here that we

are not so much interested in the absolute numbers given by the estimates than we are on the relative differences between the two periods examined. Assuming that the error sources have not changed between the periods, the estimates should give us reasonable indications of trends of the different CCN sources. Note also, that the three different CCN estimates do not "close" in the sense that the total estimate should be a sum of the nucleation and primary estimates, even if all estimates were error free. This is because we do not have an estimate for CCN produced by cloud processing (which would include most of the sulphate CCN).

The estimates for nucleation production of CCN in size ranges 50–750 nm, 100–750 nm, and 200–750 nm are presented in Table 4 as Annual Yield/cc (i.e. total number of particles per cubic centimetre produced by nucleation and growth to the respective size range within one year). For all size ranges the concentration increase per particle formation event was on the same order as the average concentration. As would be expected from the decrease of nucleation frequency and average nucleation rate between 1996–1997 and 2003–2006, the CCN production from nucleation has decreased in the 50–750 nm size range, but not very much (∼17%). Surprisingly, however, the production has clearly increased in the 100–750 nm and 200–750 nm size ranges, by ∼47% and ∼103%, respectively.

The total CCN source strengths in the different size ranges are also given in Table 4 (SS-production/cc/year). As with nucleation, the total CCN source has decreased in the smallest size range and increased in the two largest size ranges, but the relative changes are quite modest, all within 10%.

Table 5 shows our emission model results based on estimates of primary particle production in the three size ranges for years 1996, 1997, 2003, 2004 and 2005. All values have decreased from 1996–1997 to 2003–2006, with roughly 35% average reduction in all three size ranges between the two periods. Note, however, the large variances in the production rates, based on the wide variance of emission factors in the literature. We also repeated the calculation using the size distributions applied by Laaksonen et al. (2005), and obtained a similar percentage reduction although the absolute numbers (not shown) were up to an order of magnitude higher.
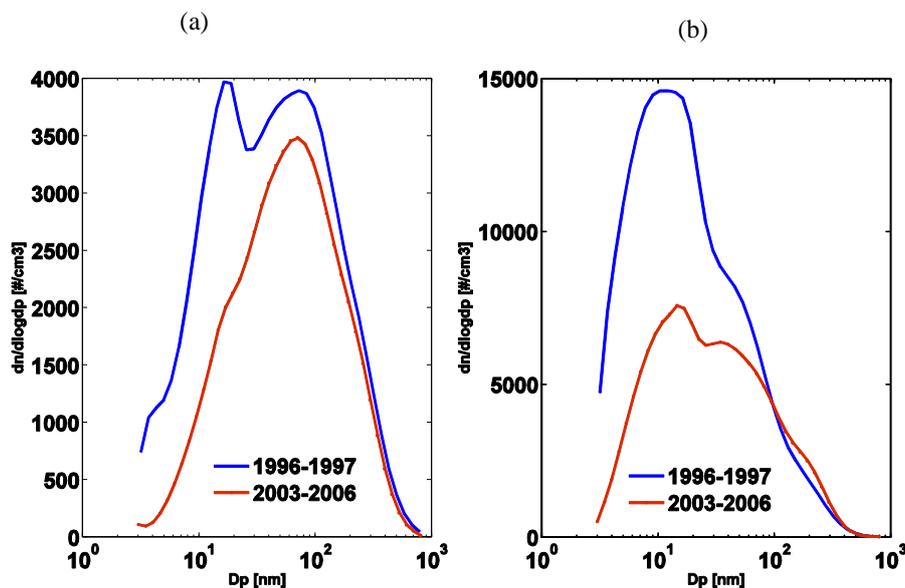
(a)   (b)

Fig. 9. Average size distributions for **(a)** nonevent days and **(b)** nucleation event days.

Table 5. Estimates of CCN number emissions shown in volume emission equivalent (cc year^{-1}) in fixed 1000 m boundary layer. CCN in size ranges 50–750 nm; 100–750 nm and 200–750 nm are shown using sector-specified emission rates (see text for details). The results are based on PM$_{2.5}$ inventories from EMEP. Years 1996 and 1997 are extrapolated from year 2000 emissions using German official PM$_{2.5}$ emission trends. The values given are the mean emission rates for all parameters tested. The ranges given in parenthesis show the differing results from using different mass-to-number emission.

	50–750 nm	100–750 nm	200–750 nm
1996*	**2.0** (0.8–3.9) **E+04**	**8.3** (6.2–11.5) **E+03**	**3.9** (1.8–4.0) **E+03**
1997*	**2.0** (0.8–3.8) **E+04**	**8.3** (6.1–11.4) **E+03**	**3.9** (1.8–3.9) **E+03**
2003	**1.5** (0.7–2.9) **E+04**	**6.2** (4.6–8.4) **E+03**	**2.1** (1.4–3.1) **E+03**
2004	**1.4** (0.6–2.8) **E+04**	**5.9** (4.4–8.2) **E+03**	**2.0** (1.3–2.8) **E+03**
2005	**1.0** (0.4–2.0) **E+04**	**4.1** (3.0–5.8) **E+03**	**1.3** (0.8–1.8) **E+03**

* Estimated from national PM$_{2.5}$ emission levels.

To summarize these results, our estimates indicate that in size ranges above 100 nm, nucleation source of CCN has increased substantially, total source has remained the same or increased slightly, and primary source has decreased clearly. In addition, it is very likely that the source from cloud processing has decreased, at least for sulphate particles. It would therefore seem that the increase of the nucleation source has more or less compensated for the decrease in primary and (cloud processed) sulphate sources.

The puzzling feature is of course that nucleation event frequency and average nucleation rate have dropped at the same time as nucleation production of CCN appears to have increased. One possible explanation is the observed increase in particle growth rates: the survival probability of freshly nucleated particles to sizes above 100 nm may have become larger, making it possible for a larger fraction of the new particles to reach CCN sizes. On the other hand, it is also possible that the same substances that cause the growth of the nucleated particles have made pre-existing particles smaller than 100 nm growing above the 100 nm limit more efficiently in 2003–2006 compared with 1996–1997. It is also possible that primary sources of sub-100nm particles have increased: after all, that would hardly be seen in the PM$_{2.5}$ emission inventories on which we based our primary CCN calculations. In order to examine these possibilities further, we first compare average size distributions from the two periods, and then present results from box model simulations of new particle contributions to CCN concentrations following "average" nucleation events in 1996–1997 and 2003–2006.

Figure 9 shows size average size distributions for strong nucleation event and nonevent days separately, for both periods. Comparing the nonevent day distributions from the two periods, it can be noted that in 1996–1997, the mode at 70 nm was about 10% higher compared with 2003–2006. A larger difference is seen in the small particle mode around 15 nm. In order to examine the reasons for the decrease of the 15 nm mode, we studied daily contour plots of aerosol size distribution evolution together with wind directions. In the contour plots, the 15 nm mode appears as sporadic (15–30 min) high concentrations, and comes from two distinct wind directions, northeast and west. The village of Melpitz, and the road leading from there to a highway is situated about 1km northeast from the measurement station, while the village of Klitzschen and the road from there to the highway is about
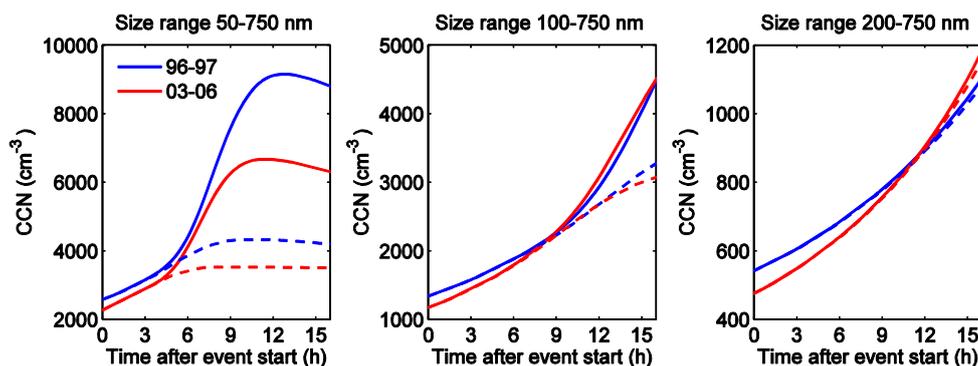
Fig. 10. UHMA simulation results of total CCN increases during "average" conditions in 1996–1997 and 2003–2006. Solid lines indicate simulations where nucleation is occurring, and dashed lines indicate otherwise identical simulations, but with no nucleation. See text for additional details.

2 km west from the site. We therefore interpret the 15 nm mode to be mainly diesel particles. The nonevent days' size distributions show no evidence of increased primary sources of sub-100 nm particles.

The nucleation day size distributions in Fig. 9 show a large difference in particle sizes below 100 nm, with higher concentrations in 1996–1997 compared with 2003–2006. This has obviously to do with the decreased nucleation rates. At sizes between about 100–300 nm, the 2003–2006 concentrations are higher, however. This is consistent with the higher CCN numbers above 100 nm calculated for the 2003–2006 period.

In order to analyze the CCN production from nucleation events, we conducted aerosol microphysics simulations using the UHMA model. Two 16-h model runs were performed for both time periods: (1) a NPF run assuming the observed annual average J_3 for two hours and letting the nucleated and background particles grow at a GR corresponding to the observed annual average value in event days, and (2) a background run without NFP but allowing the background particles grow at the same GR as in the NPF run. In both runs, the model was initialised with the annual average non-event day size distributions from the respective period, and particle loss via coagulation was simulated.

The contribution of primary sources to CCN was determined directly from the background run as the change in CCN sized particles from the start of the simulation. On the other hand, the contribution of NPF to CCN was calculated by subtracting the predicted CCN in the background run from that in the NPF run. Figure 10 shows how the total CCN numbers behave after event start in the three size ranges. Solid lines indicate events with nucleation allowed and dashed lines with nucleation disallowed. As with observations, the 1996-1997 simulations produce more particles to the 50–750 nm size range, while in the two larger size ranges the 2003–2006 concentrations are slightly higher.

The difference is smaller than in the observations; however, it should be noted that the largest CCN concentrations are produced in events with high nucleation and growth rates rather than in events with rates close to average.

Figure 11 shows the contributions from nucleated and pre-existing particles to the increasing CCN concentrations. In the smallest size range the nucleation particles dominate, while in the 100–750 nm range their contribution is less than 50%, and in the 200–750 nm range just a few percent. Again, it should be kept in mind that at higher nucleation and growth rates, the contributions from nucleated particles would likely be higher. A distinct difference between the pre-existing and nucleation particles' growth to the CCN size ranges is that the former start increasing the CCN concentrations right after the nucleation start, while it takes several hours for the nucleated particles to reach the CCN sizes. Note, that when we calculate CCN increases from ambient data, we take this into account by starting the calculations only when the nucleation "banana" reaches the size range in question. Therefore, the percentages shown in Fig. 11 actually overestimate the pre-existing particle contributions.

Taken together, our simulations show that it is possible that the 2003–2006 nucleation events have produced more CCN than the 1996–1997 events because the particle growth rates have increased even though the nucleation rates have decreased. The simulations also show that pre-existing particles do contribute to the CCN increases; however, it is difficult to quantify their contributions from the atmospheric data. The situation is even more complicated because of the fact that an unknown fraction of the pre-existing particles is not primary particles, but secondary particles formed in nucleation events in the past.
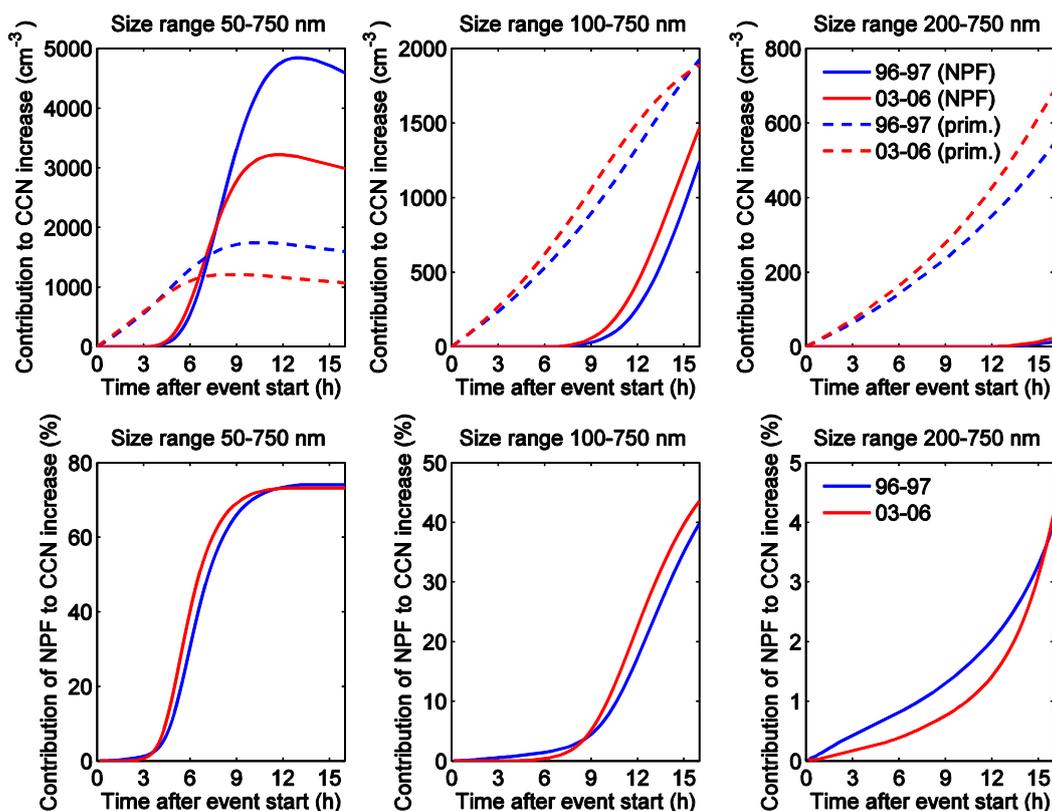
Fig. 11. UHMA simulation results of new and pre-existing particle contributions to CCN increases following "average" nucleation events in 1996–1997 and 2003–2006. See text for details.

4   Conclusions

We analysed two datasets of experimental aerosol number size distributions at the research station Melpitz, Germany, in order to evaluate the possible influence of decreasing SO_2 concentration on secondary new particle formation and on the production of cloud condensation nuclei (CCN) between 1996/1997 and 2003–2006. During the 1990s the ambient levels of SO_2 in East Germany decreased by a factor of ten as a result of socio-economic changes, leveling off after about the year 2000. Our analysis showed a significant, and concurrent drop in the frequency of new particle formation events between the two observation periods (−45%). Along with this, a decrease in the particle formation rates (−68%) was observed. The trends were statistically significant, therefore suggesting a connection between the decreasing availability of anthropogenic SO_2 and the diminishing production of new particles. A contrasting finding, however, was the increase in the growth rates of nucleated particles (+22%), suggesting that other species than H_2SO_4 dominated the particle growth. The delineation between particle formation rates and particle growth can be understood in terms of the different source types (SO_2: anthropogenic; VOCs: biogenic and anthropogenic), and was detected in Central Europe on

the basis of a multi-annual experiment also before (Birmili et al., 2003).

We also studied the effect of parameters believed to influence atmospheric nucleation such as solar radiation, CS and SO_2 concentrations. The results show that the change of SO_2 dominates over the changes of solar radiation and CS. Since sulphuric acid was not measured, we calculated a "proxy" sulphuric acid concentration making use of the fact that H_2SO_4 is formed in the reaction between SO_2 and OH-radicals, and the concentration of the latter can be correlated with intensity of solar radiation and that the CS represents H_2SO_4 loss term. The sulphuric acid proxy decreased between 1996–1997 and 2003–2006, thus supporting the conclusion that the diminishing intensity of NPF is connected to decreasing ambient levels of SO_2. The proxy correlates with measured 3 nm particle formation rates, and the slope between the logarithms of these two quantities is close to unity, in agreement with what has been observed in earlier studies of measured H_2SO_4 values and atmospheric nucleation rates. Altogether, we see strong indications that the reduction of European SO_2 pollution in Europe has caused a decrease in the production of atmospheric particles formed by nucleation and growth events.

We also examined particle concentrations in the 50–750, 100–750 nm and 200–750 nm size intervals during the hours following particle nucleation and growth events. Rather counterintuitively, our analysis suggests an increase of particle production in these size ranges despite the observed decrease in both, the frequency of nucleation events and the particle formation rates. A likely reason, confirmed by aerosol dynamics model simulations, is the enhanced particle growth rate, which was evident in the observations.

References

Alves, C., Pio, C., Carvalho, A., and Santos, C.: Atmospheric carbonaceous aerosols over grasslands of central Europe and a Boreal forest, Chemosphere, 63, 153–164, 2006.

Balkanski, Y. J.: Atmospheric residence times of continental aerosols, Ph.D. thesis, Harvard Univ., Cambridge, MA, USA, 1991.

Beilke, S. and Uhse, K.: Trend in concentration and deposition of sulfuric and nitrogenic compounds in Germany between 1982 and 1998 (translated from German), in: Jahresbericht 1998 aus dem Messnetz des Umweltbundesamtes, UBA-Texte, 66/99, Federal Environment Agency (UBA), Berlin, ISSN 0722-186X, 1999.

Birmili, W., Berresheim, H., Plass-Dülmer, C., Elste, T., Gilge, S., Wiedensohler, A., and Uhrner, U.: The Hohenpeissenberg aerosol formation experiment (HAFEX): a long-term study including size-resolved aerosol, H_2SO_4, OH, and monoterpenes measurements, Atmos. Chem. Phys., 3, 361–376, 2003, http://www.atmos-chem-phys.net/3/361/2003/.

Birmili, W., Stratmann, F., and Wiedensohler, A.: Design of a DMA-based size spectrometer for a large particle size range and stable operation, J. Aerosol Sci., 30, 549–553, 1999.

Birmili, W. and Wiedensohler, A.: New particle formation in the continental boundary layer: Meteorological and gas phase parameter influence, Geophys. Res. Lett., 27, 3325–3328, 2000.

Boy, M. and Kulmala, M.: Nucleation events in the continental boundary layer: Influence of physical and meteorological parameters, Atmos. Chem. Phys., 2, 1–16, 2002, http://www.atmos-chem-phys.net/2/1/2002/.

Ehrlich, C., Noll, G., Kalkoff, W. D., Baumback, G., and Dreiseidler, A.: PM_{10}, $PM_{2.5}$ and $PM_{1.0}$ emissions from industrial plants – Results from measurement programmes in Germany, Atmos. Environ., 41, 6236–6254, 2007.

Eisele, F. L. and McMurry, P. H.: Recent progress in understanding particle nucleation and growth, Philos. T. R. Soc. Lond. B., 352, 191–201, 1997.

Ebelt, S., Brauer, M., Cyrys, J., Tuch, T., Kreyling, W., Wichmann, H.-E., and Heinrich, J.: Air Quality in Postunification Erfurt, East Germany: Associating Changes in Pollutant Concentrations with Changes in Emissions, Environ. Health. Persp., 109, 325–333, 2001.

Engler, C., Rose, D., Wehner, B., Wiedensohler, A., Brüggemann, E., Gnauk, T., Spindler, G., Tuch, T., and Birmili, W.: Size distributions of non-volatile particle residuals ($D_p < 800$ nm) at a rural site in Germany and relation to air mass origin, Atmos. Chem. Phys., 7, 5785–5802, 2007, http://www.atmos-chem-phys.net/7/5785/2007/.

Fagerli, H., Spranger, T., and Posch, M.: Chapter 3: Acidification and eutrophication – progress towards the Gothenburg protocol target year (2010), in: EMEP Report 1/2006, Transboundary acidification, eutrophication and ground level ozone in Europe from 1990 to 2004 in support for the review of the Gothenburg Protocol, ISSN 1504-610, 2006.

Gaydos, T. M., Stanier, C. O., and Pandis, S. N.: Modeling of in situ ultrafine atmospheric particle formation in the eastern United States, J. Geophys. Res., 110, D07S12, doi:10.1029/2004JD004683, 2005.

Grini, A., Korhonen, H., Lehtinen, K. E. J., Isaksen, I., and Kulmala, M.: A combined photochemistry/aerosol dynamics model: Model development and a study of new particle formation, Boreal Environ. Res., 10, 525–541, 2005.

Hamed, A., Joutsensaari, J., Mikkonen, S., Sogacheva, L., Dal Maso, M., Kulmala, M., Cavalli, F., Fuzzi, S., Facchini, M. C., Decesari, S., Mircea, M., Lehtinen, K. E. J., and Laaksonen, A.: Nucleation and growth of new particles in Po Valley, Italy, Atmos. Chem. Phys., 7, 355–376, 2007, http://www.atmos-chem-phys.net/7/355/2007/.

Haywood, J. M. and Boucher, O.: Estimates of the direct and indirect radiative forcing due to tropospheric aerosols: A review, Rev. Geophys., 38, 513–543, 2000.

Heald, C. L., Henze, D. K., Horowitz, L. W., Feddema, J., Lamarque, J.-F., Guenther, A., Hess, P. G., Vitt, F., Goldstein, A. H., Fung, I., and Seinfeld, J. H.: Predicted change in global secondary organic aerosol concentrations in response to future climate, emissions, and land-use change, J. Geophys. Res., 113, D05211, doi:10.1029/2007JD009092, 2008.

Jeong, C. H., Hopke, P. K., Chalupa, D., and Utell, M.: Characteristics of nucleation and growth events of ultrafine particles measured in Rochester, NY, Environ. Sci. Technol., 38, 1933–1940, 2004.

Kerminen, V.-M., Anttila, T., Lehtinen, K. E. J., and Kulmala, M.: Parameterization for atmospheric new-particle formation: application to a system involving sulfuric acid and condensable water-soluble organic vapors, Aerosol. Sci. Tech., 38, 1001–1008, 2004.

Kerminen, V.-M., Lihavainen, H., Komppula, M., Viisanen, Y., and Kulmala, M.: Direct observational evidence linking atmospheric aerosol formation and cloud droplet activation, Geophys. Res. Lett., 32, L14803, doi:10.1029/2005GL023130, 2005.

Komppula, M., Sihto, S.-L., Korhonen, H., Lihavainen, H., Kerminen, V.-M., Kulmala, M., and Viisanen, Y.: New particle formation in air mass transported between two measurement sites in Northern Finland, Atmos. Chem. Phys., 6, 2811–2824, 2006, http://www.atmos-chem-phys.net/6/2811/2006/.

Korhonen, H., Lehtinen, K. E. J., and Kulmala, M.: Multicomponent aerosol dynamics model UHMA: model development and validation, Atmos. Chem. Phys., 4, 757–771, 2004, http://www.atmos-chem-phys.net/4/757/2004/.

Krüger, O., Marks, R., and Graßl, H.: Influence of pollution on cloud reflectance, J. Geophys. Res., 109, D24210, doi:10.1029/2004JD004625, 2004.

Kuang, C., McMurry, P. H., McCormick, A. V., and Eisele, F.: Dependence of nucleation rates on sulfuric acid vapor concentrations in diverse atmospheric locations, J. Geophys. Res., 13, D10209, doi:10.1029/2007JD009253, 2008.

Kuang, C., McMurry, P. H., and McCormick, A.: Determination of cloud condensation nuclei production from measured new particle formation events, Geophys. Res. Lett., 36, L09822, doi:10.1029/2009GL037584, 2009.

Kulmala, M.: How particles nucleate and grow, Science, 302, 1000–1001, 2003.

Kulmala, M., Hämeri, K., Aalto, P. P., Mäkelä, J. M., Pirjola, L., Nilsson, E. D., Buzorius, G., Rannik, U., Dal Maso, M., Seidl, W., Hoffmann, T., Jansson, R., Hansson, H.-C., Viisanen, Y., Laaksonen, A., and O'Dowd, C. D.: Overview of the international project on biogenic aerosol formation in the boreal forest (BIOFOR), Tellus, 53B, 324–343, 2001.

Kulmala, M., Laakso, L., Lehtinen, K. E. J., Riipinen, I., Dal Maso, M., Anttila, T., Kerminen, V.-M., Hõrrak, U., Vana, M., and Tammet, H.: Initial steps of aerosol growth, Atmos. Chem. Phys., 4, 2553–2560, 2004, http://www.atmos-chem-phys.net/4/2553/2004/.

Kulmala, M., Lehtinen, K. E. J., and Laaksonen, A.: Cluster activation theory as an explanation of the linear dependence between formation rate of 3 nm particles and sulphuric acid concentration, Atmos. Chem. Phys., 6, 787–793, 2006, http://www.atmos-chem-phys.net/6/787/2006/.

Kulmala, M., Petäjä, T., Mönkkönen, P., Koponen, I. K., Dal Maso, M., Aalto, P. P., Lehtinen, K. E. J., and Kerminen, V.-M.: On the growth of nucleation mode particles: source rates of condensable vapor in polluted and clean environments, Atmos. Chem. Phys., 5, 409–416, 2005, http://www.atmos-chem-phys.net/5/409/2005/.

Kulmala, M., Riipinen, I., Sipilä, M., Manninen, H. E., Petäjä, T., Junninen, H., Dal Maso, M., Mordas, G., Mirme, A., Vana, M., Hirsikko, A., Laakso, L., Harrison, M., Hanson, I., Leung, C., Lehtinen, K. E. J., and Kerminen, V.-M.: Toward direct measurement of atmospheric nucleation, Science, 318, 89–92, 2007.

Kulmala, M., Vehkamäki, H., Petäjä, T., Dal Maso, M., Lauri, A., Kerminen, V.-M., Birmili, W., and McMurry, P. H.: Formation and growth rates of ultrafine atmospheric particles: a review of observations, J. Aerosol Sci., 35, 143–176, 2004b.

Laaksonen, A., Hamed, A., Joutsensaari, J., Hiltunen, L., Cavalli, F., Junkermann, W., Asmi, A., Fuzzi, S., and Facchini, M. C.: Cloud condensation nucleus production from nucleation events at a highly polluted region, Geophys. Res. Lett., 32, 1–4, 2005.

Laaksonen, A., Kulmala, M., O'Dowd, C. D., Joutsensaari, J., Vaattovaara, P., Mikkonen, S., Lehtinen, K. E. J., Sogacheva, L., Dal

Maso, M., Aalto, P., Petäjä, T., Sogachev, A., Yoon, Y. J., Lihavainen, H., Nilsson, D., Facchini, M. C., Cavalli, F., Fuzzi, S., Hoffmann, T., Arnold, F., Hanke, M., Sellegri, K., Umann, B., Junkermann, W., Coe, H., Allan, J. D., Alfarra, M. R., Worsnop, D. R., Riekkola, M.-L., Hyötyläinen, T., and Viisanen, Y.: The role of VOC oxidation products in continental new particle formation, Atmos. Chem. Phys., 8, 2657–2665, 2008, http://www.atmos-chem-phys.net/8/2657/2008/.

Lintz, G. and Schmude, K.: Germany: Tackling the East-West divide. In Bernhard Müller, Maroš Finka and Gerd Lintz, Rise and Decline of Industry in Central and Eastern Europe: A Comparative Study of Cities and Regions in Eleven Countries, Series of Central and Eastern European Development Studies, Springer, Berlin, 81–110, 2005.

Lohmann, U. and Feichter, J.: Global indirect aerosol effects: a review, Atmos. Chem. Phys., 5, 715–737, 2005, http://www.atmos-chem-phys.net/5/715/2005/.

Lövblad, G., Tarrasön, L., Tørseth, K., and Dutchak, S.: EMEP Assessment Report Part I, European Perspective, available at http://www.emep.int, last access: 1 February 2010, Oslo, ISBN 82-7144-032-2, 2004.

Lyubovtseva, Y. S., Sogacheva, L., Dal Maso, M., Bonn, B., Keronen, P. and Kulmala, M.: Seasonal variations of trace gases, meteorological parameters, and formation of aerosols in boreal forests, Boreal Environ. Res., 10, 493–510, 2005.

Manktelow, P. T., Mann, G. W., Carslaw, K. S., Spracklen, D. V., and Chipperfield, M. P.: Regional and global trends in sulfate aerosol since the 1980s, Geophys. Res. Lett., 34, L14803, doi:10.1029/2006GL028668, 2007.

Marquardt, W., Brüggemann, E., Auel, R., Herrmann, H., and Möller, D.: Trends of pollution in rain over East Germany caused by changing emissions, Tellus, 53, 529–545, 2001.

Morawska, L., Bofinger, N. D., and Kocis, L.: Submicrometer and supermicrometer particles from diesel vehicle emissions, Environ. Sci. Technol., 32, 2033–2042, 1998.

Müller, K., Pelzing, M., Gnauk, T., Kappe, A., Teichmann, U., Spindler, G., Haferkorn, S., Jahn, Y., and Herrmann, H.: Monoterpene emissions and carbonyl compound air concentrations during the blooming period of rape (Brassica napus), Chemosphere, 49, 1247–1256, 2002.

Myhre, G., Stordal, F., Berglen, T. F., Sundet, J., and Isaksen, I. S. A.: Uncertainties in the radiative forcing due to sulfate aerosols, J. Atmos. Sci., 61, 485–498, 2004.

Napari, I., Noppel, M., Vehkamäki, H., and Kulmala, M.: Parametrization of ternary nucleation rates for H_2SO_4-NH_3-H_2O vapors, J. Geophys. Res., 107(D19), 4831, doi:10.1029/2002JD002132, 2002.

Ohlström, M. O., Lehtinen, K .E. J., Moisio, M., and Jokiniemi, J. K.: Fine-particle emissions of energy production in Finland, Atmos. Environ., 34, 3701–3711, 2000.

Pirjola, L., Laaksonen, A., Aalto, P., and Kulmala, M.: Sulfate aerosol formation in the Arctic boundary layer, J. Geophys. Res., 103, 8309–8322, 1998.

R Development Core Team R: A language and environment for statistical computing, R Foundation for Statistical Computing, Vienna, Austria, http://www.R-project.org, last access: 1 February 2010, ISBN 3-900051-07-0, 2008.

Ramanathan, V., Crutzen, P. J., Kiehl, J. T., and Rosenfeld, D.: Aerosols, climate, and the hydrological cycle, Science, 294, 2119–2124, 2001.

Ravishankara, A. R.: Heterogeneous and multiphase chemistry in the troposphere, Science, 276, 1058–1065, 1997.

Riipinen, I., Sihto, S.-L., Kulmala, M., Arnold, F., Dal Maso, M., Birmili, W., Saarnio, K., Teinilä, K., Kerminen, V.-M., Laaksonen, A., and Lehtinen, K. E. J.: Connections between atmospheric sulphuric acid and new particle formation during QUEST III-IV campaigns in Heidelberg and Hyytiälä, Atmos. Chem. Phys., 7, 1899–1914, 2007,
http://www.atmos-chem-phys.net/7/1899/2007/.

Rohrer, F. and Berresheim, H.: Strong correlation between levels of tropospheric hydroxyl radical and solar ultraviolet radiation, Nature, 442, 184–187, 2006.

Sekiguchi, M., Nakajima, T., Suzuki, K., Kawamoto, K., Higurashi, A., Rosenfeld, D., Sano, I., and Mukai, S.: A study of the direct and indirect effects of aerosols using global satellite data sets of aerosol and cloud parameters, J. Geophys. Res., 108(D22), 4699, doi:10.1029/2002JD003359, 2003.

Sihto, S.-L., Kulmala, M., Kerminen, V.-M., Dal Maso, M., Petäjä, T., Riipinen, I., Korhonen, H., Arnold, F., Janson, R., Boy, M., Laaksonen, A., and Lehtinen, K. E. J.: Atmospheric sulphuric acid and aerosol formation: implications from atmospheric measurements for nucleation and early growth mechanisms, Atmos. Chem. Phys., 6, 4079–4091, 2006,
http://www.atmos-chem-phys.net/6/4079/2006/.

Spindler, G., Müller, K. , Brüggemann, E., Gnauk, T., and Herrmann, H.: Long-term size-segregated characterization of PM_{10}, $PM_{2.5}$, and PM_1 at the IfT research station Melpitz downwind of Leipzig (Germany) using high and low-volume filter samplers, Atmos. Environ., 38, 5333–5347, 2004.

Stanier, C. O., Khlystov, A. Y., and Pandis, S. N.: Nucleation events during the Pittsburgh Air Quality Study: Description and relation to key meteorological, gas phase, and aerosol parameters, Aerosol Sci. Tech., 38, 253–264, 2004.

Tunved, P., Hansson, H.-C., Kerminen, V.-M., Ström, J., Dal Maso, M., Lihavainen, H., Viisanen, Y., Aalto, P. P., Komppula, M., and Kulmala, M.: High natural aerosol loading over boreal forests, Science, 312, 261–263, 2006.

Tunved, P., Korhonen, H., Ström, J., Hansson, H.-C., Lehtinen, K. E. J., and Kulmala, M.: Is nucleation capable of explaining observed aerosol integral number during southerly transport over Scandinavia?, Tellus, 58B, 129–140, 2006.

Vehkamäki, H., Kulmala, M., Napari, I., Lehtinen, K. E. J., Timmreck, C., Noppel, M., and Laaksonen, A.: An improved parameterization for sulfuric acid/water nucleation rates for tropospheric and stratospheric conditions, J. Geophys. Res., 107(D22), 4622, doi:10.1029/2002JD002184, 2002.

Vestreng, V., Myhre, G., Fagerli, H., Reis, S., and Tarrasón, L.: Twenty-five years of continuous sulphur dioxide emission reduction in Europe, Atmos. Chem. Phys., 7, 3663–3681, 2007,
http://www.atmos-chem-phys.net/7/3663/2007/.

Vestreng, V., Rigler, E., Adams, M., Kindbom, K., Pacyna, J. M., Denier van der Gon, H., Reis, S., and Travnikov, O.: Inventory review 2006, Emission data reported to LRTAP and NEC Directive, Stage 1, 2 and 3 review and Evaluation of inventories of HM and POPs, EMEP/MSC-W Technical Report 1/2006, available at http://www.emep.int, last access: 1 February 2010, ISSN 1504-6179, 2006.

Weber, R. J., Marti, J. J., McMurry, P. H., Eisele, F. L., Tanner, D. J., and Jefferson, A.: Measurements of new particle formation and ultrafine particle growth rates at a clean continental site, J. Geophys. Res., D102, 4375–4385, 1997.

Weber, R. J., McMurry, P. H., Mauldin, R. L., Tanner, D. J., Eisele, F. L., Clarke, A. D., and Kapustin, V. N.: New particle formation in the remote troposphere: A comparison of observations at various sites, Geophys. Res. Lett., 26, 307–310, 1999.

Wehner, B. and Wiedensohler, A.: Long term measurements of submicrometer urban aerosols: statistical analysis for correlations with meteorological conditions and trace gases, Atmos. Chem. Phys., 3, 867–879, 2003,
http://www.atmos-chem-phys.net/3/867/2003/.

Wehner, B., Petäjä, T., Boy, M., Engler, C., Birmili, W., Tuch, T., Wiedensohler, A., and Kulmala, M.: The contribution of sulfuric acid and non-volatile compounds on the growth of freshly formed atmospheric aerosols, Geophys. Res. Lett., 32, L17810, doi:10.1029/2005GL023827, 2005.

Zhang, Q., Stanier, C. O., Canagaratna, M., Jayne, J., Worsnop, D. R., Pandis, S., and Jimenez, J.: Insights into the chemistry of new particle formation and growth events in Pittsburgh based on aerosol mass spectrometry, Environ. Sci. Technol., 38, 4797–4809, 2004.